

# <sup>1</sup> Imposed form in the Early Acheulean? Evidence from Gona, <sup>2</sup> Afar, Ethiopia

Dietrich Stout\* Cheng Liu† Antoine Muller‡ Michael J. Rogers§  
Silesh Semaw¶

2023-09-24

## Abstract

TBD.

**Keywords:** Gona; TBD; TBD; TBD; TBD; TBD; TBD

## **9    Contents**

10	<b>1 Introduction</b>	2
11	1.1 Identifying design . . . . .	2
12	1.2 Measuring artifact form and modification . . . . .	6
13	1.3 The Early Acheulean at Gona . . . . .	8
14	<b>2 Materials and Methods</b>	9
15	2.1 Materials . . . . .	9
16	2.2 Methods . . . . .	9
17	<b>3 Results</b>	11
18	3.1 Measurement Validation . . . . .	11
19	3.2 Classification Validation . . . . .	13
20	3.3 Effects of Reduction on Shape . . . . .	14
21	<b>4 Discussion</b>	15
22	<b>References</b>	16

\*Department of Anthropology, Emory University, Atlanta, GA, USA; dwstout@emory.edu

<sup>†</sup>Department of Anthropology, Emory University, Atlanta, GA, USA; raylc1996@outlook.com

<sup>‡</sup>Institute of Archaeology, Mount Scopus, The Hebrew University of Jerusalem, Jerusalem, Israel; [antoine.muller@mail.huji.ac.il](mailto:antoine.muller@mail.huji.ac.il)

<sup>§</sup>Department of Anthropology, Southern Connecticut State University, New Haven, CT, USA; rogersml@southernct.edu

<sup>¶</sup>Centro Nacional de Investigación sobre la Evolución Humana (CENIEH), Burgos, Spain; sileshi.semaw@cenieh.es

23 **1 Introduction**

24 The imposition of intended form on artifacts has long been viewed as a watershed in human  
25 cognitive and cultural evolution and is most commonly associated with the emergence of “Large  
26 Cutting Tools” (LCTs) in the Early Acheulean (Holloway, 1969; Isaac, 1976; Kuhn, 2021). However,  
27 this interpretation of Acheulean LCTs as intentionally designed artifacts remains controversial.  
28 Alternative proposals range from the possibility that LCTs were unintended by-products of flake  
29 production (Moore & Perston, 2016; Noble & Davidson, 1996) to the suggestion that their form  
30 was “at least partly under genetic control” (Corbey et al., 2016). Even accepting that LCT form  
31 was to some extent intended, there is substantial disagreement over the specificity of design.  
32 Some analyses have indicated that shape variation in Acheulean handaxes is largely a result of  
33 resharpening (Iovita & McPherron, 2011; McPherron, 2000) whereas others find form to be unre-  
34 lated to reduction intensity and more likely to reflect normative expectations of what handaxes  
35 should look like (García-Medrano et al., 2019; Shipton & Clarkson, 2015b; Shipton & White, 2020).  
36 Such debates about shape of Acheulean LCTs may appear narrowly technical but have broad  
37 relevance for evolutionary questions including the origins of human culture (Corbey et al., 2016;  
38 Shipton & Clarkson, 2015b; Tennie et al., 2017), language (Stout & Chaminade, 2012), teaching  
39 (Gärdenfors & Höglberg, 2017), brain structure (Hecht et al., 2015), and cognition (Stout et al.,  
40 2015; Wynn & Coolidge, 2016). To examine these questions, we studied the complete collection  
41 of Early Acheulean flaked pieces from 5 sites at Gona Project Area and compared them with  
42 Oldowan cores from 2 published sites at Gona. By comparing shape variation to measures of  
43 flaking intensity and patterning, we sought to identify technological patterns that might reveal  
44 intent.

45 **1.1 Identifying design**

46 There is a broad consensus that refined handaxes and cleavers from the later Acheulean resulted  
47 from procedurally elaborate, skill intensive, and socially learned production strategies (Caruana,  
48 2020; García-Medrano et al., 2019; Moore, 2020; Sharon, 2009; Shipton, 2019; Stout et al., 2014)  
49 although debate over the presence of explicit, culturally transmitted shape preferences continues  
50 (Iovita & McPherron, 2011; Moore, 2020; Shipton & White, 2020; Wynn & Gowlett, 2018). There is  
51 much less agreement regarding the less heavily worked and formally standardized LCTs typical  
52 of the earliest Acheulean (Beyene et al., 2013; Diez-Martín et al., 2015; Lepre et al., 2011; Semaw

53 et al., 2018; Torre & Mora, 2018). Such forms continue to occur with variable frequency in later  
54 time periods (McNabb & Cole, 2015), and may be especially prevalent in eastern Asia (Li et al.,  
55 2021). Although formal types have been recognized in the Early Acheulean and are commonly  
56 used to describe assemblages, many workers now see a continuum of morphological variation  
57 (Duke et al., 2021; Kuhn, 2021; Presnyakova et al., 2018) including the possibility that simple  
58 flake production remained an important (Shea, 2010) or even primary (Moore & Perston, 2016)  
59 purpose of Early Acheulean large core reduction.

60 Typologically, LCTs are differentiated from Mode 1 pebble cores on the basis of size (>10cm) and  
61 shape (elongation and flattening) (e.g., Isaac, 1977). This consistent production of large, flat, and  
62 elongated cores in the Achuelean has long been thought to reflect the pursuit of desired functional  
63 and ergonomic properties for hand-held cutting tools (Wynn & Gowlett, 2018). Unplanned  
64 flaking can sometimes produce cores that fall into the LCT shape range (Moore & Perston, 2016)  
65 and this is one possible explanation of the relatively small “probifaces” that occur in low  
66 frequencies in Oldowan assemblages (Isaac & Isaac, 1997). However, the Early Acheulean is  
67 clearly distinguished from the Oldowan by the production of larger artifacts necessitating the  
68 procurement and exploitation of larger raw material clasts. Although studies of handaxe variation  
69 often focus on shape rather than size, this shift is an important aspect of artifact design with  
70 relevance to both production and function.

71 Production of larger tools was accomplished either through a novel process of detaching and  
72 working Large Flake Blanks (LFBs) from boulder cores or simply by using larger cobble and slab  
73 cores (Isaac, 1969; Semaw et al., 2018; Torre & Mora, 2018). Both may involve similar flaking  
74 “strategies” (e.g., bifacial or multifacial exploitation) to those present in the Oldowan (Duke et al.,  
75 2021) but require more forceful percussion to detach larger flakes. This increases the perceptual  
76 motor difficulty of the task (Stout, 2002) and in many cases may have been accomplished using  
77 different percussive techniques and supports (Semaw et al., 2009). These new challenges would  
78 have increased raw material procurement (Shea, 2010) and learning costs (Pargeter et al., 2019) as  
79 well as the risk of serious injury (Gala et al., 2023) associated with tool production. This strongly  
80 implies intentional pursuit of offsetting functional benefits related to size increase. These likely  
81 included tool ergonomics and performance (Key & Lycett, 2017) as well as flake generation,  
82 resharpening, and reuse potential (Shea, 2010). Early Acheulean LCT production is thus widely  
83 seen as a part of shifting hominin behavioral ecological strategies including novel resources and

84 mobility patterns (Linares Matás & Yravedra, 2021; Rogers et al., 1994).

85 The degree of intentional design reflected in the shape of Early Acheulean LCTs is more difficult to  
86 determine. For example, LFB production using a simple “least effort” bifacial/discoidal strategy  
87 will tend to generate predominantly elongated (side or end struck) flakes (Toth, 1982) whether  
88 or not this is an intentional design target. Similarly, the difficulty of flaking relatively spherical  
89 cobbles (Toth, 1982) might bias initial clast selection and subsequent reduction toward flat and  
90 elongated shapes even in the absence of explicit design targets. On the other hand, it has been  
91 argued that the shape of Early Acheulean LFBs was intentionally predetermined using core  
92 preparation techniques (Torre & Mora, 2018) and many researchers perceive efforts at intentional  
93 shaping in the organization of flake scars on Early Acheulean handaxes and picks (Beyene et  
94 al., 2013; Diez-Martín et al., 2015; Duke et al., 2021; Lepre et al., 2011; Semaw et al., 2009; Torre  
95 & Mora, 2018). To date, however, the identification of Early Acheulean shaping has generally  
96 relied on qualitative assessment by lithic analysts. Such assessment may in fact be reliable, but is  
97 subject to concerns about potential selectivity, bias, and/or overinterpretation (Davidson, 2002;  
98 Moore & Perston, 2016). Notably, a 3-dimensional morphometric (3DGM) study by Presnyakova,  
99 et al. (2018) concluded that LCT shape variation in the Okote Member (~1.4 mya) at Koobi Fora  
100 was largely driven by reduction intensity rather than different knapping strategies. However, this  
101 study did not directly address the presence/absence of design targets constraining the observed  
102 range of variation.

103 In later Acheulean contexts, reduction intensity effects are commonly equated with resharpening  
104 and seen as an alternative to intentional form imposition (McPherron, 2000). Across heavily-  
105 worked and relatively standardized LCT assemblages (e.g., Shipton & White, 2020), a *lack* of asso-  
106 ciation between morphology and reduction intensity has been used as an argument-by-elimination  
107 for the presence of imposed morphological norms or “mental templates” (García-Medrano et  
108 al., 2019; Shipton et al., 2023; Shipton & Clarkson, 2015b). However, in the less heavily-worked  
109 and more heterogeneous assemblages typical of the early Acheulean (Kuhn, 2021), it is equally  
110 plausible that increasing reduction intensity would reflect degree of primary reduction rather  
111 than subsequent resharpening (Archer & Braun, 2010). In this case, reduction intensity effects  
112 on morphology would have the opposite interpretation: more reduction should result in closer  
113 approximation of a desired form if such were present. For example, Beyene, et al. (2013) found  
114 that increasing flake scar counts were associated with increasing handaxe refinement through

<sup>115</sup> time at Konso, Ethiopia, which may reflect a more general trend in the African Acheulean ([Shipton, 2018](#)).<sup>116</sup>

<sup>117</sup> Interpretive approaches address this quandary by “reading” the organization of scars on individual pieces to infer intent, but an adequate method to objectively quantify these insights has yet to be developed. Current measures of reduction intensity, such as the scar density index (SDI) ([Clarkson, 2013](#)), are designed to estimate total mass removed from a core and are reasonably effective ([Lombao et al., 2023](#)). However, mass removal was not the objective of Paleolithic flaking. Indeed, knapping efficiency is usually conceived as generating an outcome while *minimizing* required mass removal. This is true whether the desired outcome is a useful flake, a rejuvenated edge, or a particular core morphology. In simple flake production, mass removed is probably a good reflection of the completeness of exploitation (“exhaustion”) of cores and may have implications for required skill ([Pargeter et al., 2023; Toth, 1982](#)) as well as raw material economy ([Reeves et al., 2021; Shick, 1987](#)). However, in core shaping and resharpening, mass removal would typically represent an energetic and raw material cost to be minimized, and might even interfere with function ([Key, 2019](#)). Without further information, relationships between artifact shape and reduction intensity are thus open to conflicting interpretations as evidence of intentional design or its absence.<sup>131</sup>

<sup>132</sup> Li, et al. ([2015](#)) proposed a Flaked Area Index (FAI) as an alternative to SDI as a measure of reduction intensity, arguing that its validity is supported by an observed correlation ( $r=0.424$ ) with SDI. However, they also explain that “flaked area does not necessarily relate to the number of flake scars...a small number of large scars can produce a large area of scar coverage, and conversely, a large number of small scars can produce a small area of scar coverage.” (p. 6). We suggest that what FAI actually captures is the spatial extent modifications to the surface of a core. It is thus complementary to the measure of volume reduction provided by SDI and provides additional information to inform technological interpretations. For example, a correlation between FAI and artifact form without any effect of SDI would suggest a focus on “least-effort” shape imposition whereas the opposite pattern would be consistent with relatively intense resharpening of spatially restricted areas on the core. A lack of shape correlation with either measure would be expected for simple debitage with no morphological targets whereas a strong correlation with both would indicate a highly “designed” form achieved through extensive morphological and volumetric transformation. In the current study we thus considered SDI and FAI together in order to evaluate<sup>145</sup>

<sup>146</sup> evidence of intentional shaping in the early Acheulean of Gona.

## <sup>147</sup> 1.2 Measuring artifact form and modification

<sup>148</sup> Three-dimensional scanning and geometric morphometric (3DGM) methods are increasingly  
<sup>149</sup> common in the study of LCT form and reduction intensity ([Archer & Braun, 2010](#); [Caruana, 2020](#);  
<sup>150</sup> [Li et al., 2015, 2021](#); [Lycett et al., 2006](#); [Presnyakova et al., 2018](#); [Shipton & Clarkson, 2015b](#)).  
<sup>151</sup> These methods provide high-resolution, coordinate-based descriptions of artifact form including  
<sup>152</sup> detailed information about whole object geometric relations that is not captured by conventional  
<sup>153</sup> linear measures ([Shott & Trail, 2010](#)). This includes measures of surface area used to compute  
<sup>154</sup> both SDI and FAI measures ([Clarkson, 2013](#); [Li et al., 2015](#)). At the time of writing, however, 3D  
<sup>155</sup> scans are available for only a small number of Gona artifacts, including 33 of the Oldowan and  
<sup>156</sup> Acheulean flaked pieces used in this study ([Figure 1](#)). Despite continuing improvements, 3DGM  
<sup>157</sup> methods still impose additional costs in terms of data collection and processing time as well as  
<sup>158</sup> required equipment, software, and training. Importantly, 3DGM methods cannot be applied to  
<sup>159</sup> pre-existing photographic and metric data sets (e.g., [Marshall et al., 2002](#)), including available  
<sup>160</sup> data from Gona. For this reason, and to better understand the relative costs and benefits of  
<sup>161</sup> 3DGM more generally, we sought to test the degree to which conventional measurements can  
<sup>162</sup> approximate 3DGM methods and produce reliable results by directly comparing our conventional  
<sup>163</sup> measures with 3DGM analysis of the 33 available scans.

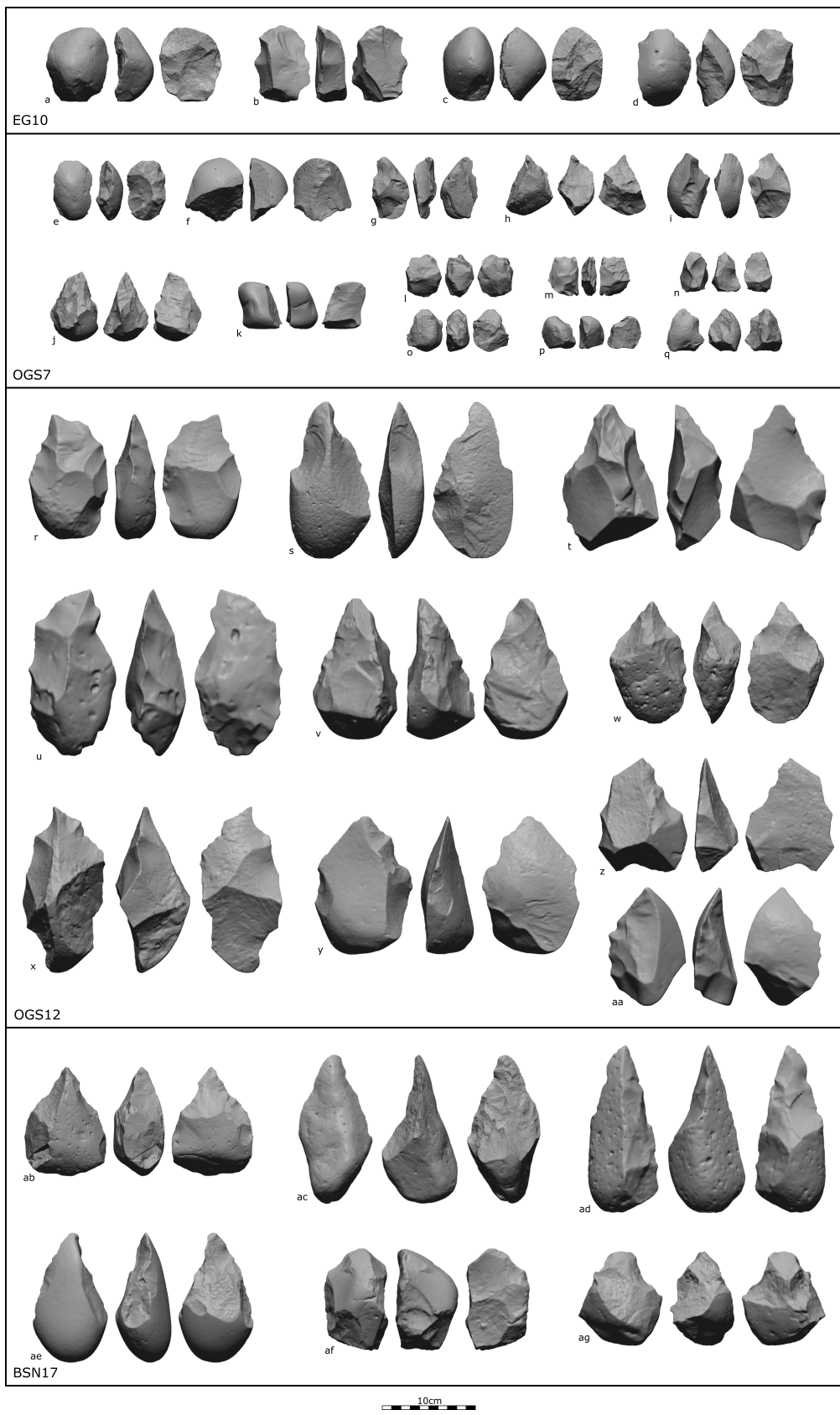


Figure 1: 3D Artifact scans from Gona used in this study.

164 For our study, we are specifically concerned with the accurate description of morphological  
165 variation and estimation of artifact surface and flaked areas. With respect to morphology, we  
166 were encouraged by the fact that aspects of form variation relevant to our research question (i.e.,  
167 core elongation, flattening, and pointedness) are relatively simple to describe using sparse data.  
168 3DGM studies of LCTs collect vast amounts of shape data but may discard upward of 50% of the  
169 observed variation in order to focus on two or three interpretable principal components. Across  
170 studies, these PCs consistently correspond to basic features like elongation, relative thickness,  
171 pointedness, and position of maximum thickness that also emerge from lower-resolution spatial  
172 data (Archer & Braun, 2010; García-Medrano et al., 2019; Lycett et al., 2006) and studies employing  
173 linear measures rather than spatial coordinates (Crompton & Gowlett, 1993; Pargeter et al., 2019).  
174 There is less evidence that conventional methods can accurately estimate artifact surface and  
175 flaked areas. Clarkson (2013) advocated the use of 3D surface area measures as more accurate  
176 than estimation from linear measures (e.g., surface area of a rectangular prism defined by artifact  
177 dimensions). However, he also found that the error introduced by the linear approach was a  
178 highly systematic, isometric overestimation of surface area and that results correlated with direct  
179 3D measures with an impressive  $r^2 = 0.944$  and no effect of variation in core shape. Insofar as  
180 it is variation in the relationship between surface area and flaking intensity that is of interest,  
181 rather than absolute artifact size, such systematic overestimation may not be problematic. Similar  
182 concerns apply to the estimation of flaked area. Traditionally, such estimates have been done “by  
183 eye” as a percentage of the total artifact surface (e.g., Dibble et al., 2005). Such estimations have  
184 been found to be reasonably accurate when compared to 3D methods, but with the potential for  
185 substantial error on individual artifacts (Lin et al., 2010). The accuracy of by-eye estimation has  
186 yet to be systematically studied in Early Stone Age cores like those from Gona.

### 187 1.3 The Early Acheulean at Gona

188 Early Acheulean sites in the Gona Project area are distributed over a wide area within the Dana  
189 Aoule North (DAN), Ounda Gona South (OGS), and Busidima North (BSN) drainages in the  
190 Busidima Formation (Quade et al., 2004) and range in age from approximately 1.7 to 1.2 mya  
191 (Semaw et al., 2018). The specific sites included in the current analysis are DAN-5, OGS-5, OGS-12,  
192 and BSN-17, all estimated to ca. 1.7 – 1.4 mya by stratigraphic position in the Gona sequence  
193 (Quade et al., 2008; Semaw et al., 2020). The Busidima Formation accumulated through fluvial  
194 deposition by the ancestral Awash River (Type I context) and its smaller tributary channels (Type

195 II context) (Quade et al., 2004, 2008). Oldowan sites at Gona all occur in Type I sediments,  
196 indicating channel bank/margin (OGS-7) or proximal floodplain (EG-10, EG-12) contexts close  
197 to the large, hetero-lithic clasts available from point bars in the axial river channel (Quade et al.,  
198 2004; Stout et al., 2005). Acheulean sites continue to occur in Type I contexts (BSN-17, DAN-5)  
199 but are also found in Type II sediments (OGS-5, OGS-12,) reflecting increased utilization of large  
200 perennial tributaries to the ancestral Awash River (Quade et al., 2008). Clasts locally available  
201 in these tributaries were relatively small, implying that the large flakes and cobbles used to  
202 produce Acheulean artifacts were initially sourced from the axial river. A similar pattern of habitat  
203 diversification and increasing lithic transport distances has been described at other sites and  
204 may be typical of the early Acheulean (Hay, 1976; Linares Matás & Yravedra, 2021; Rogers et  
205 al., 1994). As with other early (i.e. >1.0 mya (Presnyakova et al., 2018; Stout, 2011)) Acheulean  
206 assemblages, the Gona collections include numerous “crudely made” handaxes and picks on large  
207 flake blanks and cobbles, as well as large (> 10cm) unmodified flakes, flaked pieces interpreted  
208 typo-technologically as Mode 1 cores (see Figure 1af), and smallerdebitage (Semaw et al., 2018;  
209 Semaw et al., 2020).

## 210 2 Materials and Methods

### 211 2.1 Materials

#### 212 2.1.1 Archaeological Sample

213 Artifact collections analyzed here include *in situ* pieces excavated from intact stratigraphic  
214 contexts and surface pieces systematically collected from the sediments eroding from these  
215 layers. Surface pieces are included because the current technological analysis does not require  
216 more precise spatial association, stratigraphic, and chronological control. Our sample comprises  
217 the total collection of flaked pieces (Isaac & Isaac, 1997) and large (>10 cm) detached pieces from  
218 each site, regardless of typo-technological interpretation.

### 219 2.2 Methods

#### 220 2.2.1 Artifact Classification

221 Artifacts were classified according to initial form (pebble/cobble, detached piece, or indetermi-  
222 nate), presence/absence of retouch, technological interpretation (“Mode 1” core vs. “Mode 2”

223 LCT), and archaeological context (Oldowan vs. Early Acheulean sites). LCTs were additionally  
224 classified as handaxes, knives, or picks following definitions from Kleindienst (1962). The validity  
225 of technological interpretations and typological classifications was assessed through cluster  
226 analysis based on artifact shape and reduction intensity variables.

227 **2.2.2 Artifact Measurement**

228 Conventional linear measures capture the direction (e.g., length > breadth) but not the location of  
229 geometric relations (e.g., position of maximum breadth). We address this by collecting linear mea-  
230 sures defined by homologous semi-landmarks. All artifacts were oriented along their maximum  
231 dimension, which was measured and defined as “length.” The next largest dimension orthogonal  
232 to length was used to define the plane of “breadth,” with the dimension orthogonal to this plane  
233 defined as “thickness” Width ( $W_1, W_2, W_3$ ) and thickness ( $T_1, T_2, T_3$ ) measures were then collected  
234 at 25%, 50%, and 75% of length, oriented so that 25% Width > 75% Width. To partition variation  
235 in shape from variation in size, we divided all linear measures by the geometric mean (Lycett et  
236 al., 2006). GM-transformed variables were then submitted to a Principal Components Analysis  
237 (covariance matrix) to identify the main dimensions of shape variation.

238 Our semi-landmark measurement system allowed us to improve on the prism-based surface area  
239 formula ( $2LW + 2LT + 2WT$ ) by using our 7 recorded dimensions to more tightly fit three prisms  
240 around the artifact:  $SA = W_1T_1 + 2(.33L * W_1) + 2(.33L * T_1) + 2(.33L * W_2) + 2(.33L * T_2) + 2(.33L *$   
241  $W_3) + 2(.33L * T_3) + W_3T_3$ . Surface area calculated in this way correlates with mass<sup>2/3</sup> at  $r^2 = 0.947$   
242 in our sample. Calculated surface area was then used to derive the Scar Density Index: SDI =  
243 number of flake scars > 1cm per unit surface area (Clarkson, 2013; Shipton & Clarkson, 2015a).  
244 The Flaked Area Index (FAI: flaked area divided by total surface area) (Li et al., 2015) was estimated  
245 directly “by eye” as a percentage of the total artifact surface.

246 **2.2.3 3D Methods**

247 Artifact scans (N=33) were cleaned, smoothed, and re-meshed using MeshLab. The 3D triangular  
248 mesh of each scan was computed using Kazhdan and Hoppe’s (2013) method of screened Poisson  
249 surface reconstruction in MeshLab. 3DGM analysis was conducted using the AGMT3-D program  
250 of Herzlinger and Grosman (2018). Artifacts were automatically oriented according to the axis  
251 of least asymmetry, then manually oriented in the interests of standardization with the length,

width, and thickness dimensions defined by the longest axis, followed by the next two longest axes perpendicular to the first. The wider end of the artifacts was positioned as the proximal end (base), and more protruding surfaces were oriented towards the user in the first orthogonal view. Then, a grid of 200 homologous semi-landmarks were overlain on each artifact's surface. Generalized Procrustes and Principal Component analyses were then undertaken to explore the shape variability of the sample. The surface area of each artifact was calculated using the *Artifact3-D* program of Grosman et al. (2022). *Artifact3-D* was also used to automatically identify the flake scar boundaries and compute each scar's surface area, using the scar analysis functions of Richardson et al. (2014).

#### 2.2.4 Analyses

Measurement Validation: To assess the adequacy of shape descriptions based on our linear measures, we directly compared these with shape as quantified by 3D methods on the 33 artifacts for which scans are available. GM-transformed linear measures from these 33 artifacts were submitted to a variance-covariance matrix PCA. PCs with an eigenvalue greater than the mean were retained for analysis and the results compared qualitatively (morphological interpretation of PCs) and quantitatively (correlation of artifact factor scores) to 3D results. Accuracy of surface area and flaked area estimates was also assessed by correlation with 3D results.

## 3 Results

### 3.1 Measurement Validation

A PCA on GM transformed linear measures the 33 artifacts identified two PCs accounting for 75.6% of the variance. Linear-PC1 (Eigenvalue = 0.189) explained 55.2% of the variance. Factor loadings (**Table 1**) for Linear-PC1 reflect artifact elongation (i.e., an anti-correlation of length vs. distal width and thickness). This A PCA on GM transformed linear measures the 33 artifacts identified two PCs accounting for 75.6% of the variance. Linear-PC1 (Eigenvalue = 0.189) explained 55.2% of the variance. Factor loadings (**Table 1**) for Linear-PC1 reflect artifact elongation (i.e., an anti-correlation of length vs. distal width and thickness). This closely parallels the length vs. width and thickness tradeoff captured by 3DGM-PC1 (Figure 3a) and is reflected in a tight correlation of artifact scores produced by the two PCs ( $r = 0.903$ ,  $p < 0.001$ , Figure 3c). Comparison with

Table 1: Component loadings for linear metric PCs .

Linear.metrics..GM.transformed.	Linear.PC1	Linear.PC2
Length	0.989	-0.107
W1	0.303	0.350
W2	0.403	0.767
W3	-0.176	0.790
T1	-0.135	-0.679
T2	-0.369	-0.623
T3	-0.607	-0.282

conventional shape ratios (Table 2) similarly indicates that both Linear-PC1 and 3DGM-PC1 largely capture variation in artifact elongation. A second factor (Linear-PC2, eigenvalue = 0.07) explained an additional 20.4% of variance. This factor was less strongly correlated with its 3DGM counterpart (3DGM-PC2;  $r = 0.344$ ,  $p = 0.050$ ) probably because Linear-PC2 describes anticorrelated variation in width and thickness (i.e., broad and flat vs. thick and pointed; Table 1) whereas 3DGM-PC2 more purely isolates convergence (Figure 3a). The remainder of the shape variability explained by Linear-PC2 is captured by higher order 3DGM-PCs like 3DGM-PC3 to 5, which comprise the contribution of the left and right lateral margins to relative thickness. Use of high-resolution, coordinate-based scan data thus generates PCs that identify more specific shape attributes, but the underlying morphological variability captured by the linear and 3D analyses remains similar. Together, 3DGM-PC2 ( $r = 0.344$ ,  $p = 0.050$ ), 3DGM-PC3 ( $r = -0.416$ ,  $p = 0.016$ ), 3DGM-PC4 ( $r = 0.458$ ,  $p = 0.007$ ), and 3DGM-PC5 ( $r = -0.352$ ,  $p = 0.044$ ) correlate well with Linear-PC2 (Figure 3c), cumulatively capturing whether the items are broad and flat or thick and pointed. A stepwise regression ( $r^2=0.625$ ,  $F(4,28)=11.697$ ,  $p<0.001$ , Probability-of-F-to-enter  $\leq 0.050$ ; Probability-of-F-to-remove  $\geq 0.100$ ) with Linear-PC2 as the dependent variable retained all four of these 3DGM-PCs as significant predictors.

We thus concluded that linear measures are adequate to capture relevant shape variation and proceeded with a PCA on our full sample. We identified two PCs accounting for 80.0% of the variance. PC1 (Eigenvalue = 0.216) explained 56.4% of the variance. Factor loadings (Table 2) for PC1 reflect artifact flatness (i.e., an anti-correlation of length and width vs. thickness) such that higher values indicate relatively thinner pieces. PC2 (Eigenvalue = 0.090) explained 23.6% of the variance. Factor loadings (Table 2) show that PC2 captures artifact convergence or “pointedness” (i.e., an anti-correlation of tip width with length and butt thickness) such that higher values

303 indicate shorter, less pointed forms.

304 We also tested the validity of our two reduction measures, SDI and FAI. In agreement with Clarkson  
305 (2013), we found that surface area estimated from caliper measures displayed a strong correlation  
306 with ( $r^2=0.975$ ,  $p < 0.001$ ) but linear over-estimation of ( $\beta = 1.58$ ) 3DGM surface area (Figure 4a).  
307 This results in a systematic underestimation of SDI that scales with core size (Figure 4b). However,  
308 a simple correction of the caliper estimate (dividing by the slope, 1.58) eliminates surface area  
309 over-estimation (mean difference = 256mm<sup>2</sup> [ $<1.7\%$  of mean],  $p=0.040$ ) and produces SDI values  
310 that agree with 3DGM ( $r^2=0.975$ ,  $p < 0.001$ ,  $\beta = 0.98$ ) (Figure 4c). We thus proceeded to apply this  
311 correction to surface area estimates in the full sample. Insofar as these relationships are driven by  
312 basic geometry, we expect these methods (including correction) to be generalizable to other ESA  
313 assemblages.

### 314 3.2 Classification Validation

315 We first conducted a stepwise DFA on all flaked pieces (n=192) with inferred technological Mode  
316 (one vs. two) as the grouping variable and PCs 1 and 2, corrected SDI (cSDI), and FAI as the  
317 independent variables. All variables were retained, yielding one canonical DF (eigenvalue=1.825,  
318 Wilks Lambda = 0.354,  $p < 0.001$ ) which correctly classified 93.8% of artifacts. We thus accepted  
319 the validity of classification by Mode in our sample and employed this distinction in subsequent  
320 analyses. There was no discernable difference in discriminant scores for Mode 1 cores from  
321 Oldowan (n=37) vs. Acheulean (n=39) contexts (,  $p = 0.746$ ). Mode 1 cores from Oldowan contexts  
322 (n=37) do include 10 (27%) small, retouched flakes. Only one retouched flake from an Acheulean  
323 context was classified by the DFA as a Mode 1 core. This piece, typologically classified as a “knife”,  
324 is the smallest (93mm) retouched flake in the Acheulean sample. When retouched flakes are  
325 excluded from the comparison, there are no significant differences in shape between Mode 1 cores  
326 from Oldowan and Achuelean contexts. Interestingly, however, Acheulean Mode 1 cobble-cores  
327 are much larger (mean weight 480g vs. 186g, Cohen’s d=1.137,  $p < 0.001$ ) and less heavily reduced  
328 (mean cSDI 0.057 vs. 0.103, Cohen’s d = -0.884,  $p < 0.001$ ) despite having similar FAI (mean 0.52  
329 vs. 0.46, Cohen’s d=0.271,  $p=0.266$ ).

330 Next, we conducted a stepwise DFA on all flaked Mode 2 pieces (i.e. excluding unmodified large  
331 flakes, n = 115) with typology (handaxe, pick, knife) as the grouping variable and the same four  
332 independent variables. Both shape PCs and FAI were retained, while cSDI was not entered.

333 This produced two DFs (DF1: Eigenvalue=1.536, 91.3% of variance; DF2: Eigenvalue = 0.146,  
334 8.7% of variance; Wilks Lambda = 0.344; p<0.001) which correctly classified 71.3% of artifacts.  
335 Inspection of DF coefficients shows that DF1 captures an inverse correlation between flaked area  
336 and pointedness (Linear-PC2) whereas DF2 captures a positive relationship between flaked area  
337 and elongation (Linear-PC2). A bivariate plot (Figure 5) illustrates the fact that DF1 captures  
338 a range of variation from pointed, heavily-worked picks, through handaxes, to knives, with  
339 substantial overlap between adjacent types (Table 2). As an intermediate type, “handaxes” were  
340 correctly classified only 43.9% of the time. In agreement with others (Duke et al., 2021; Kuhn,  
341 2021; Presnyakova et al., 2018) we conclude that these typological labels artificially partition a  
342 continuum of variation and abandon them in subsequent analyses.

### 343 3.3 Effects of Reduction on Shape

344 To assess the influence of flake removals on core form, we examined the association between  
345 our reduction measures (cSDI and FAI) and core shape (PC1, PC2). In the complete sample of  
346 flaked pieces (n=192), we observed weak but significant effects of cSDI ( $r=-0.294$ ,  $p < 0.001$ ) and  
347 FAI ( $r=-0.294$ ,  $p < 0.001$ ) on PC1(flatness) and of FAI only on PC2(pointedness) ( $r=-0.436$ ,  $p < 0.001$ ).  
348 However, it is clear that these overall effects conflate different trends in Mode 1 vs. Mode 2 cores,  
349 as well as in cores executed on flake vs. pebble/cobble bases. Within categories, we observed no  
350 significant effects of cSDI whereas FAI had variable relationships with core form.

351 In Mode 1 cores, a weak negative effect of FAI on PC2(pointedness) ( $n = 76$ ,  $\beta = -0.006$ ,  $r=0.240$ ,  
352  $p= 0.037$ ) suggests that increasing extent of modification tends to slightly increase pointedness  
353 (Figure 6a). No effects of FAI on PC1 (flatness) or of SDIc on either PC approach significance. FAI  
354 and SDIc are moderately correlated ( $\beta=0.001$ ,  $r=0.524$ ,  $p < 0.001$ ), an effect that reflects increases  
355 in the upper limit of scar density values as flaked area increases (i.e., flaked area constrains  
356 maximum cSDI: Figure 6b).

357 In Mode 2 cores ( $n=115$ ), reduction measures have different effects depending on initial blank  
358 form. In general, the contrast between flat, lightly-worked flake bases and rounder, more-heavily  
359 worked cobble bases tends to inflate relationships between FAI and core shape (Figure 7c,d).  
360 Mode 2 cobble cores ( $n=37$ ) display a negative effect of FAI on PC1(Flatness) ( $\beta=-0.011$ ,  $r=0.367$ ,  $p$   
361 = 0.026), no effect of FAI on pointedness, and no association between FAI and cSDI ( $r=0.141$ ,  $p =$   
362 0.406). Flake cores ( $n=69$ ) show negative effects of FAI on PC1(Flatness) ( $\beta=-0.007$ ,  $r=0.284$ ,  $p =$

363 0.018) and, more strongly, PC2(pointedness) ( $\beta=-0.019$ ,  $r=0.443$ ,  $p < 0.001$ ). Flake cores show a  
364 small but significant positive effect of FAI on cSDI that, in contrast to Mode 1 cores, represents  
365 actual covariance rather than simply a relaxation of constraint (i.e. both upper and lower limits of  
366 cSDI increase with FAI).

367 Comparison of Mode 2 flake cores with unmodified large flakes from Achuelean contexts (n=35)  
368 shows that ranges of shape variation substantially overlap but that flaking generally reduces  
369 both PC1(flatness) and PC2(pointedness). In fact, regressions of PC1 and PC2 on FAI show y-  
370 intercepts that closely approximate unmodified flake mean values (0.852 vs. 0.774 and 0.693  
371 vs. 0.594, respectively) and significantly negative slopes as FAI increases (Figure 9).

372 A small number of Mode 2 cores (n=9) were so heavily modified (mean FAI=89%, range 65-100)  
373 that the blank form could not be determined. These heavily worked “indeterminate” cores tend  
374 to show similar PC1(flatness) and PC2(pointedness) values to cobble-base cores (i.e. thicker and  
375 more pointed than flake cores; Figure x). They also appear to follow general trends of shape  
376 change with increasing FAI observed across base types (Figure 10).

## 377 4 Discussion

378 Following the criteria we proposed in the Introduction, Large Flake base cores from Acheulean  
379 contexts show evidence of design. Importantly, “design” in this context is understood as “design in  
380 four dimensions” sensu Kuhn (2021). Increasing FAI is associated with progressive narrowing (i.e.,  
381 decreasing PC1) and convergence (decreasing PC2) whereas cSDI is not. This indicates that the  
382 size and non-overlapping placement of flake removals drives shape change, rather than simply  
383 the removal of mass in general as might be expected from conventional models of resharpening  
384 (?). The fact that cSDI nevertheless correlates with FAI is consistent with relatively light (number  
385 of scars per piece ranges from 2 to 17 with a mean of 6.94) and spatially distributed re-touching  
386 involving relatively little overlap between scars. Such a pattern could be produced by intentional  
387 imposition of a design target or “mental template” or a more procedural/functional bias in favor of  
388 establishing cutting edges at one end of the long axis. In the absence of effective thinning/volume  
389 management techniques, this will lead to rapid narrowing/thickening of the piece overall and  
390 especially at the “tip.” This is consistent with differences between flaked vs. unmodified large  
391 flakes and furthers the point that blank production already can be conceived as a process of

392 “design” – many unmodified flakes may have been similar in shape and just as useful as many  
393 retouched tools.

394 This contrasts with reduction of Mode 1 cores. Unexpectedly, FAI did have an effect to increase  
395 convergence. However, this effect was substantially weaker than seen in LFB Acheulean cores  
396 and may simply reflect the fact that reduction is unlikely to be perfectly symmetrical and our  
397 orienting protocol guarantees that one end is always more pointed than the other unless they  
398 are precisely equal in breath. In support of this “byproduct” interpretation, the relationship  
399 between FAI and cSDI is essentially what one would expect from knapping unconstrained by any  
400 systematic core-shaping strategy (greater flaked area can, but does not necessarily, accommodate  
401 a greater number of flake scars)

402 Our most complicated results come from Mode 2 cobble cores. Evidence of intentional shaping is  
403 limited: FAI has a moderate effect on PC1(flatness) and no effect on pointedness. Furthermore,  
404 there is no association between FAI and cSDI cobble cores display a greater range of cSDI values.  
405 Instead, FAI is strongly correlated with scar size (mean scar length: n=33, r=.588, P<0.001; Figure  
406 11). Together, this suggests that the removal of large flakes in particular increases FAI and tends  
407 to narrow the piece. We propose that this pattern may actually indicate that at least some cobble  
408 cores were precisely that: cores for the generation of LFBs. Given the difficulty of working relatively  
409 spherical cobbles, we expect that knappers would have chosen elongated and/or tabular cobbles.  
410 Attempts to maximize potential flake dimensions would naturally lead to removals along the long  
411 axis rather than at either end. This hypothesis was suggested by informal “experiential” knapping  
412 by the lead author with Gona cobbles, during which LFB production produced pick like forms  
413 as a byproduct. In support of the plausibility of this hypothesis, the maximum scars length on  
414 Gona Mode 2 cobble cores substantially overlaps with the size of unmodified large flakes from  
415 Acheulean contexts. It is also possible that cobble cores might begin as cores for LFB production  
416 and then be finished into core tools in their own right. These possibilities have major implications  
417 for understanding the occurrence and apparent morphological stability ([Beyene et al., 2013](#)) of  
418 “picks” throughout the African Acheuelan but remains to be tested.

## 419 References

- 420 Archer, W., & Braun, D. R. (2010). Variability in bifacial technology at Elandsfontein, Western cape,  
421 South Africa: a geometric morphometric approach. *Journal of Archaeological Science*, 37(1),

- 422 201–209. <https://doi.org/10.1016/j.jas.2009.09.033>
- 423 Beyene, Y., Katoh, S., WoldeGabriel, G., Hart, W. K., Uto, K., Sudo, M., Kondo, M., Hyodo, M.,  
424 Renne, P. R., Suwa, G., & Asfaw, B. (2013). The characteristics and chronology of the earliest  
425 Acheulean at Konso, Ethiopia. *Proceedings of the National Academy of Sciences*, 110(5), 1584–  
426 1591. <https://doi.org/10.1073/pnas.1221285110>
- 427 Caruana, M. V. (2020). South African handaxes reloaded. *Journal of Archaeological Science: Reports*, 34, 102649. <https://doi.org/10.1016/j.jasrep.2020.102649>
- 428 Clarkson, C. (2013). Measuring core reduction using 3D flake scar density: a test case of changing  
429 core reduction at Klasies River Mouth, South Africa. *Journal of Archaeological Science*, 40(12),  
430 4348–4357. <https://doi.org/10.1016/j.jas.2013.06.007>
- 431 Corbey, R., Jagich, A., Vaesen, K., & Collard, M. (2016). The acheulean handaxe: More like a bird's  
432 song than a beatles' tune? *Evolutionary Anthropology: Issues, News, and Reviews*, 25(1), 6–19.  
433 <https://doi.org/10.1002/evan.21467>
- 434 Crompton, R. H., & Gowlett, J. A. J. (1993). Allometry and multidimensional form in Acheulean  
435 bifaces from Kilombe, Kenya. *Journal of Human Evolution*, 25(3), 175–199. <https://doi.org/10.1006/jhev.1993.1043>
- 436 Davidson, I. (2002). *The Finished Artefact Fallacy: Acheulean Hand-axes and Language Origins* (A.  
437 Wray, Ed.; pp. 180–203). Oxford University Press. <https://rune.une.edu.au/web/handle/1959.11/1837>
- 438 Dibble, H. L., Schurmans, U. A., Iovita, R. P., & McLaughlin, M. V. (2005). The measurement and  
439 interpretation of cortex in lithic assemblages. *American Antiquity*, 70(3), 545–560. <https://doi.org/10.2307/40035313>
- 440 Diez-Martín, F., Sánchez Yustos, P., Uribelarrea, D., Baquedano, E., Mark, D. F., Mabulla, A.,  
441 Fraile, C., Duque, J., Díaz, I., Pérez-González, A., Yravedra, J., Egeland, C. P., Organista, E., &  
442 Domínguez-Rodrigo, M. (2015). The Origin of The Acheulean: The 1.7 Million-Year-Old Site of  
443 FLK West, Olduvai Gorge (Tanzania). *Scientific Reports*, 5(1), 17839. <https://doi.org/10.1038/srep17839>
- 444 Duke, H., Feibel, C., & Harmand, S. (2021). Before the Acheulean: The emergence of bifacial  
445 shaping at Kokiselei 6 (1.8 Ma), West Turkana, Kenya. *Journal of Human Evolution*, 159, 103061.  
446 <https://doi.org/10.1016/j.jhevol.2021.103061>
- 447 Gala, N., Lycett, S. J., Bebber, M. R., & Eren, M. I. (2023). The Injury Costs of Knapping. *American  
448 Antiquity*, 1–19. <https://doi.org/10.1017/aaq.2023.27>

- 454 García-Medrano, P., Ollé, A., Ashton, N., & Roberts, M. B. (2019). The Mental Template in Handaxe  
455 Manufacture: New Insights into Acheulean Lithic Technological Behavior at Boxgrove, Sussex,  
456 UK. *Journal of Archaeological Method and Theory*, 26(1), 396–422. <https://doi.org/10.1007/s10816-018-9376-0>
- 458 Gärdenfors, P., & Höglberg, A. (2017). The archaeology of teaching and the evolution of homo  
459 docens. *Current Anthropology*, 58(2), 188–208. <https://doi.org/10.1086/691178>
- 460 Grosman, L., Muller, A., Dag, I., Goldgeier, H., Harush, O., Herzlinger, G., Nebenhaus, K., Valetta,  
461 F., Yashuv, T., & Dick, N. (2022). Artifact3-D: New software for accurate, objective and efficient  
462 3D analysis and documentation of archaeological artifacts. *PLOS ONE*, 17(6), e0268401.  
463 <https://doi.org/10.1371/journal.pone.0268401>
- 464 Hay, R. L. (1976). *Geology of the Olduvai Gorge: A study of sedimentation in a semiarid basin.*  
465 University of California Press.
- 466 Hecht, E. E., Gutman, D. A., Khriesheh, N., Taylor, S. V., Kilner, J. M., Faisal, A. A., Bradley, B. A.,  
467 Chaminade, T., & Stout, D. (2015). Acquisition of Paleolithic toolmaking abilities involves  
468 structural remodeling to inferior frontoparietal regions. *Brain Structure & Function*, 220(4),  
469 2315–2331. <https://doi.org/10.1007/s00429-014-0789-6>
- 470 Herzlinger, G., & Grosman, L. (2018). AGMT3-D: A software for 3-D landmarks-based geometric  
471 morphometric shape analysis of archaeological artifacts. *PLOS ONE*, 13(11), e0207890. <https://doi.org/10.1371/journal.pone.0207890>
- 473 Holloway, R. L. (1969). Culture: A human domain. *Current Anthropology*, 10(4), 395–412. <https://www.jstor.org/stable/2740553>
- 475 Iovita, R., & McPherron, S. P. (2011). The handaxe reloaded: A morphometric reassessment  
476 of Acheulian and Middle Paleolithic handaxes. *Journal of Human Evolution*, 61(1), 61–74.  
477 <https://doi.org/10.1016/j.jhevol.2011.02.007>
- 478 Isaac, G. L. (1969). Studies of early culture in east africa. *World Archaeology*, 1(1), 1–28. <https://doi.org/10.1080/00438243.1969.9979423>
- 480 Isaac, G. L. (1976). Stages of Cultural Elaboration in the Pleistocene: Possible Archaeological  
481 Indicators of the Development of Language Capabilities. *Annals of the New York Academy of  
482 Sciences*, 280(1), 275–288. <https://doi.org/10.1111/j.1749-6632.1976.tb25494.x>
- 483 Isaac, G. L. (1977). *Olongesailie: Archaeological studies of a middle pleistocene lake basin in kenya.*  
484 University of Chicago Press.
- 485 Isaac, G. L., & Isaac, B. (1997). *The stone artefact assemblages: A comparative study* (p. 262299).

- 486 Kazhdan, M., & Hoppe, H. (2013). Screened poisson surface reconstruction. *ACM Transactions on*  
487 *Graphics*, 32(3), 29:129:13. <https://doi.org/10.1145/2487228.2487237>
- 488 Key, A. J. M. (2019). Handaxe shape variation in a relative context. *Comptes Rendus Palevol*, 18(5),  
489 555–567. <https://doi.org/10.1016/j.crpv.2019.04.008>
- 490 Key, A. J. M., & Lycett, S. J. (2017). Influence of Handaxe Size and Shape on Cutting Efficiency: A  
491 Large-Scale Experiment and Morphometric Analysis. *Journal of Archaeological Method and*  
492 *Theory*, 24(2), 514–541. <https://doi.org/10.1007/s10816-016-9276-0>
- 493 Kleindienst, M. R. (1962). Components of the East African Acheulian assemblage: An analytic  
494 approach. In G. Mortelmans & J. A. E. Nenquin (Eds.), *Actes du IVeme Congres Panafricain*  
495 *de Préhistoire et de L'étude du Quaternaire* (Vol. 40, pp. 81–105). Musée Royal de l'Afrique  
496 Centrale.
- 497 Kuhn, S. L. (2021). *The evolution of paleolithic technologies*. Routledge.
- 498 Lepre, C. J., Roche, H., Kent, D. V., Harmand, S., Quinn, R. L., Brugal, J.-P., Texier, P.-J., Lenoble,  
499 A., & Feibel, C. S. (2011). An earlier origin for the Acheulian. *Nature*, 477(7362), 82–85.  
500 <https://doi.org/10.1038/nature10372>
- 501 Li, H., Kuman, K., & Li, C. (2015). Quantifying the Reduction Intensity of Handaxes with 3D  
502 Technology: A Pilot Study on Handaxes in the Danjiangkou Reservoir Region, Central China.  
503 *PLOS ONE*, 10(9), e0135613. <https://doi.org/10.1371/journal.pone.0135613>
- 504 Li, H., Lei, L., Li, D., Lotter, M. G., & Kuman, K. (2021). Characterizing the shape of Large Cutting  
505 Tools from the Baise Basin (South China) using a 3D geometric morphometric approach.  
506 *Journal of Archaeological Science: Reports*, 36, 102820. <https://doi.org/10.1016/j.jasrep.2021.102820>
- 508 Lin, S. C. H., Douglass, M. J., Holdaway, S. J., & Floyd, B. (2010). The application of 3D laser  
509 scanning technology to the assessment of ordinal and mechanical cortex quantification in  
510 lithic analysis. *Journal of Archaeological Science*, 37(4), 694–702. <https://doi.org/10.1016/j.jas.2009.10.030>
- 512 Linares Matás, G. J., & Yravedra, J. (2021). ‘We hunt to share’: Social dynamics and very large  
513 mammal butchery during the oldowan–acheulean transition. *World Archaeology*, 53(2), 224–  
514 254. <https://doi.org/10.1080/00438243.2022.2030793>
- 515 Lombao, D., Rabuñal, J. R., Cueva-Temprana, A., Mosquera, M., & Morales, J. I. (2023). Establishing  
516 a new workflow in the study of core reduction intensity and distribution. *Journal of Lithic*  
517 *Studies*, 10(2), 25 p. <https://doi.org/10.2218/jls.7257>

- 518 Lycett, S. J., Cramon-Taubadel, N. von, & Foley, R. A. (2006). A crossbeam co-ordinate caliper  
519 for the morphometric analysis of lithic nuclei: a description, test and empirical examples of  
520 application. *Journal of Archaeological Science*, 33(6), 847–861. <https://doi.org/10.1016/j.jas.2005.10.014>
- 522 Marshall, G., Dupplaw, D., Roe, D., & Gamble, C. (2002). *Lower palaeolithic technology, raw  
523 material and population ecology (bifaces)*. Archaeology Data Service. <https://doi.org/10.5284/1000354>
- 525 McNabb, J., & Cole, J. (2015). The mirror cracked: Symmetry and refinement in the Acheulean  
526 handaxe. *Journal of Archaeological Science: Reports*, 3, 100–111. <https://doi.org/10.1016/j.jasrep.2015.06.004>
- 528 McPherron, S. P. (2000). Handaxes as a Measure of the Mental Capabilities of Early Hominids.  
529 *Journal of Archaeological Science*, 27(8), 655–663. <https://doi.org/10.1006/jasc.1999.0467>
- 530 Moore, M. W. (2020). Hominin Stone Flaking and the Emergence of ‘Top-down’ Design in Human  
531 Evolution. *Cambridge Archaeological Journal*, 30(4), 647–664. <https://doi.org/10.1017/S0959774320000190>
- 533 Moore, M. W., & Perston, Y. (2016). Experimental Insights into the Cognitive Significance of Early  
534 Stone Tools. *PLOS ONE*, 11(7), e0158803. <https://doi.org/10.1371/journal.pone.0158803>
- 535 Noble, W., & Davidson, I. (1996). *Human evolution, language and mind: A psychological and  
536 archaeological inquiry*. Cambridge University Press.
- 537 Pargeter, J., Khreisheh, N., & Stout, D. (2019). Understanding stone tool-making skill acquisition:  
538 Experimental methods and evolutionary implications. *Journal of Human Evolution*, 133,  
539 146–166. <https://doi.org/10.1016/j.jhevol.2019.05.010>
- 540 Pargeter, J., Liu, C., Kilgore, M. B., Majoe, A., & Stout, D. (2023). Testing the Effect of Learning  
541 Conditions and Individual Motor/Cognitive Differences on Knapping Skill Acquisition. *Journal  
542 of Archaeological Method and Theory*, 30(1), 127–171. <https://doi.org/10.1007/s10816-022-09592-4>
- 544 Presnyakova, D., Braun, D. R., Conard, N. J., Feibel, C., Harris, J. W. K., Pop, C. M., Schlager, S.,  
545 & Archer, W. (2018). Site fragmentation, hominin mobility and LCT variability reflected in  
546 the early Acheulean record of the Okote Member, at Koobi Fora, Kenya. *Journal of Human  
547 Evolution*, 125, 159–180. <https://doi.org/10.1016/j.jhevol.2018.07.008>
- 548 Quade, J., Levin, N. E., Simpson, S. W., Butler, R., McIntosh, W. C., Semaw, S., Kleinsasser, L.,  
549 Dupont-Nivet, G., Renne, P., & Dunbar, N. (2008). *The geology of gona, afar, ethiopia* (J. Quade

- 550 & J. G. Wynn, Eds.; p. 131). Geological Society of America.
- 551 Quade, J., Levin, N., Semaw, S., Stout, D., Renne, P., Rogers, M., & Simpson, S. (2004). Paleoenvirons-  
552 ments of the earliest stone toolmakers, gona, ethiopia. *GSA Bulletin*, 116(11-12), 1529–1544.  
553 <https://doi.org/10.1130/B25358.1>
- 554 Reeves, J. S., Braun, D. R., Finestone, E. M., & Plummer, T. W. (2021). Ecological perspectives on  
555 technological diversity at Kanjera South. *Journal of Human Evolution*, 158, 103029. <https://doi.org/10.1016/j.jhevol.2021.103029>
- 557 Richardson, E., Grosman, L., Smilansky, U., & Werman, M. (2014). *Extracting scar and ridge*  
558 *features from 3D-scanned lithic artifacts* (A. Chrysanthi, C. Papadopoulos, D. Wheatley, G. Earl,  
559 I. Romanowska, P. Murrieta-Flores, & T. Sly, Eds.; pp. 83–92). Amsterdam University Press.  
560 <https://doi.org/10.1017/9789048519590.010>
- 561 Rogers, M. J., Harris, J. W. K., & Feibel, C. S. (1994). Changing patterns of land use by Plio-  
562 Pleistocene hominids in the Lake Turkana Basin. *Journal of Human Evolution*, 27(1), 139–158.  
563 <https://doi.org/10.1006/jhev.1994.1039>
- 564 Semaw, S., Rogers, M. J., Cáceres, I., Stout, D., & Leiss, A. C. (2018). *The Early Acheulean 1.6–1.2 Ma*  
565 *from Gona, Ethiopia: Issues related to the Emergence of the Acheulean in Africa* (R. Gallotti & M.  
566 Mussi, Eds.; pp. 115–128). Springer International Publishing. [https://doi.org/10.1007/978-3-319-75985-2\\_6](https://doi.org/10.1007/978-3-<br/>567 319-75985-2_6)
- 568 Semaw, S., Rogers, M. J., Simpson, S. W., Levin, N. E., Quade, J., Dunbar, N., McIntosh, W. C.,  
569 Cáceres, I., Stinchcomb, G. E., Holloway, R. L., Brown, F. H., Butler, R. F., Stout, D., & Everett, M.  
570 (2020). Co-occurrence of acheulian and oldowan artifacts with homo erectus cranial fossils  
571 from gona, afar, ethiopia. *Science Advances*, 6(10), eaaw4694. [https://doi.org/10.1126/sciadv.aaw4694](https://doi.org/10.1126/sciadv.<br/>572 .aaw4694)
- 573 Semaw, S., Rogers, M., & Stout, D. (2009). *The Oldowan-Acheulian Transition: Is there a “Developed*  
574 *Oldowan” Artifact Tradition?* (M. Camps & P. Chauhan, Eds.; pp. 173–193). Springer. [https://doi.org/10.1007/978-0-387-76487-0\\_10](https://doi.org/10.1007/978-0-387-76487-0_10)
- 576 Sharon, G. (2009). Acheulian giant-core technology: A worldwide perspective. *Current Anthropol-*  
577 *ogy*, 50(3), 335–367. <https://doi.org/10.1086/598849>
- 578 Shea, J. J. (2010). *Stone Age Visiting Cards Revisited: A Strategic Perspective on the Lithic Technology*  
579 *of Early Hominin Dispersal* (J. G. Fleagle, J. J. Shea, F. E. Grine, A. L. Baden, & R. E. Leakey, Eds.;  
580 pp. 47–64). Springer Netherlands. [https://doi.org/10.1007/978-90-481-9036-2\\_4](https://doi.org/10.1007/978-90-481-9036-2_4)
- 581 Shick, K. D. (1987). Modeling the formation of Early Stone Age artifact concentrations. *Journal of*

- 582      *Human Evolution*, 16(7), 789–807. [https://doi.org/10.1016/0047-2484\(87\)90024-8](https://doi.org/10.1016/0047-2484(87)90024-8)
- 583      Shipton, C. (2018). Biface Knapping Skill in the East African Acheulean: Progressive Trends and  
584      Random Walks. *African Archaeological Review*, 35(1), 107–131. <https://doi.org/10.1007/s10437-018-9287-1>
- 585      Shipton, C. (2019). The Evolution of Social Transmission in the Acheulean. In K. A. Overmann & F.  
586      L. Coolidge (Eds.), *Squeezing Minds From Stones: Cognitive Archaeology and the Evolution of  
587      the Human Mind* (pp. 332–354). Oxford University Press.
- 588      Shipton, C., & Clarkson, C. (2015a). Flake scar density and handaxe reduction intensity. *Journal of  
589      Archaeological Science: Reports*, 2, 169–175. <https://doi.org/10.1016/j.jasrep.2015.01.013>
- 590      Shipton, C., & Clarkson, C. (2015b). Handaxe reduction and its influence on shape: An experimen-  
591      tal test and archaeological case study. *Journal of Archaeological Science: Reports*, 3, 408–419.  
592      <https://doi.org/10.1016/j.jasrep.2015.06.029>
- 593      Shipton, C., Groucutt, H. S., Scerri, E., & Petraglia, M. D. (2023). Uniformity and diversity in  
594      handaxe shape at the end of the acheulean in southwest asia. *Lithic Technology*, 0(0), 1–14.  
595      <https://doi.org/10.1080/01977261.2023.2225982>
- 596      Shipton, C., & White, M. (2020). Handaxe types, colonization waves, and social norms in the  
597      British Acheulean. *Journal of Archaeological Science: Reports*, 31, 102352. <https://doi.org/10.1016/j.jasrep.2020.102352>
- 598      Shott, M. J., & Trail, B. W. (2010). Exploring new approaches to lithic analysis: Laser scanning and  
599      geometric morphometrics. *Lithic Technology*, 35(2), 195–220. <https://doi.org/10.1080/01977261.2010.11721090>
- 600      Stout, D. (2002). Skill and cognition in stone tool production: An ethnographic case study from  
601      irian jaya. *Current Anthropology*, 43(5), 693–722. <https://doi.org/10.1086/342638>
- 602      Stout, D. (2011). Stone toolmaking and the evolution of human culture and cognition. *Philoso-  
603      sophical Transactions of the Royal Society B: Biological Sciences*, 366(1567), 1050–1059. <https://doi.org/10.1098/rstb.2010.0369>
- 604      Stout, D., Apel, J., Commander, J., & Roberts, M. (2014). Late Acheulean technology and cognition  
605      at Boxgrove, UK. *Journal of Archaeological Science*, 41, 576–590. <https://doi.org/10.1016/j.jas.2013.10.001>
- 606      Stout, D., & Chaminade, T. (2012). Stone tools, language and the brain in human evolution.  
607      *Philosophical Transactions of the Royal Society B: Biological Sciences*, 367(1585), 75–87. <https://doi.org/10.1098/rstb.2011.0099>
- 608      <https://doi.org/10.1098/rstb.2011.0099>
- 609      <https://doi.org/10.1098/rstb.2011.0099>
- 610      <https://doi.org/10.1098/rstb.2011.0099>
- 611      <https://doi.org/10.1098/rstb.2011.0099>
- 612      <https://doi.org/10.1098/rstb.2011.0099>
- 613      <https://doi.org/10.1098/rstb.2011.0099>

- 614 Stout, D., Hecht, E., Khriesheh, N., Bradley, B., & Chaminade, T. (2015). Cognitive Demands of  
615 Lower Paleolithic Toolmaking. *PLOS ONE*, 10(4), e0121804. <https://doi.org/10.1371/journal.pone.0121804>
- 616
- 617 Stout, D., Quade, J., Semaw, S., Rogers, M. J., & Levin, N. E. (2005). Raw material selectivity of the  
618 earliest stone toolmakers at Gona, Afar, Ethiopia. *Journal of Human Evolution*, 48(4), 365–380.  
619 <https://doi.org/10.1016/j.jhevol.2004.10.006>
- 620 Tennie, C., Premo, L. S., Braun, D. R., & McPherron, S. P. (2017). Early stone tools and cultural  
621 transmission: Resetting the null hypothesis. *Current Anthropology*, 58(5), 652–672. <https://doi.org/10.1086/693846>
- 622
- 623 Torre, I. de la, & Mora, R. (2018). Technological behaviour in the early Acheulean of EF-HR  
624 (Olduvai Gorge, Tanzania). *Journal of Human Evolution*, 120, 329–377. <https://doi.org/10.1016/j.jhevol.2018.01.003>
- 625
- 626 Toth, N. (1982). *The stone technologies of early hominids at koobi fora, kenya: An experimental  
627 approach* [PhD thesis]. <https://www.proquest.com/docview/303067974/abstract/305CC66DA94A43EEPQ/1>
- 628
- 629 Wynn, T., & Coolidge, F. L. (2016). Archeological insights into hominin cognitive evolution.  
630 *Evolutionary Anthropology: Issues, News, and Reviews*, 25(4), 200–213. <https://doi.org/10.1002/evan.21496>
- 631
- 632 Wynn, T., & Gowlett, J. (2018). The handaxe reconsidered. *Evolutionary Anthropology: Issues,  
633 News, and Reviews*, 27(1), 21–29. <https://doi.org/10.1002/evan.21552>